



Supplement of

Reliability of resilience estimation based on multi-instrument time series

Taylor Smith et al.

Correspondence to: Taylor Smith (tasmith@uni-potsdam.de)

The copyright of individual parts of the supplement might differ from the article licence.

14 **Synthetic Data Parameterization**

Sensor	Time frame	Relative Reliability
SSMI	1987-01-01 to 2002-04-01	0.7
TMI	1997-12-01 to 2015-04-01	0.5
WindSat	2003-02-01 to 2012-07-01	0.44
AMSR-E	2002-06-01 to 2011-10-01	0.88
AMSR-2	2012-07-01 onwards	1

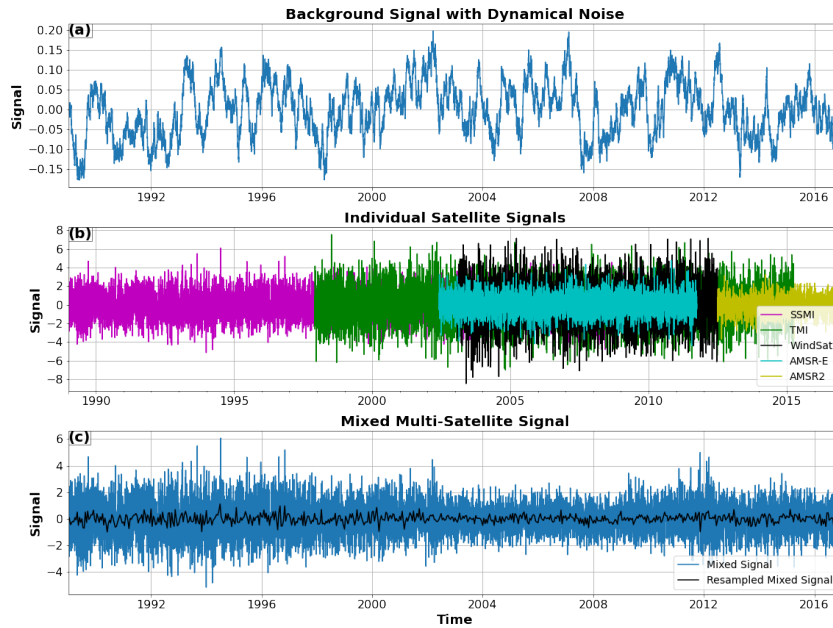
15 **Table S1.** Time frame and relative reliability for the satellites making up the VODCA data
16 set. AMSR-2 is considered to be the most reliable (value of 1), with WindSat being the least
17 (value of 0.44). Values calculated roughly from the variability of the underlying data sets, and
18 to match aggregated synthetic patterns with those of the global VODCA patterns in lag-one
19 autocorrelation and variance.

Sensor	Time frame	Relative Reliability
NOAA 9F	1985-02-01 to 1988-09-01	0.87
NOAA 11H	1988-09-01 to 1994-09-30	1
NOAA 9F-d	1994-09-01 to 1995-01-01	0.88
NOAA 14J	1995-01-01 to 2000-11-01	0.79
NOAA 16L	2000-11-01 to 2003-12-01	0.85
NOAA 17M	2003-12-01 to 2009-01-01	0.83
NOAA 18N	2005-08-01 onwards	0.7
NOAA 19N	2009-06-01 onwards	0.65

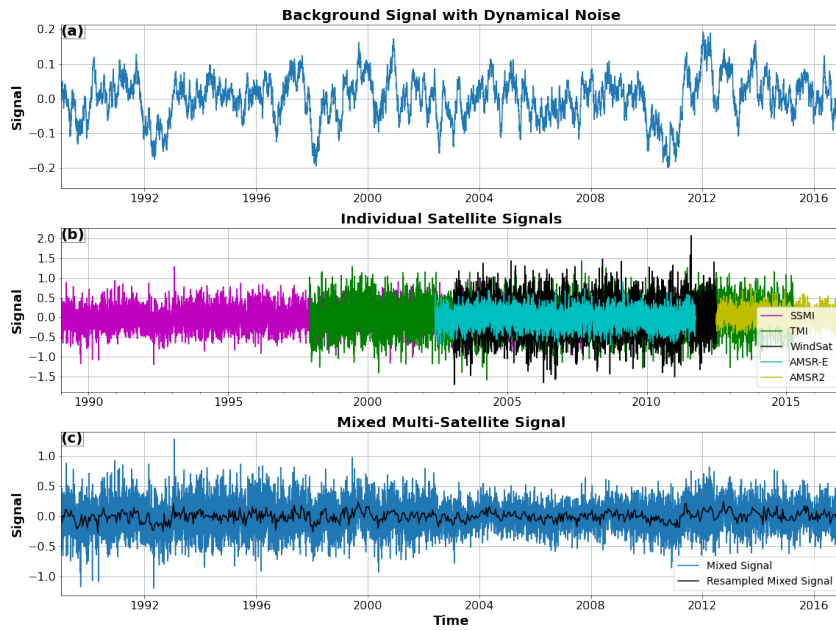
20 **Table S2.** Time frame and relative reliability for the satellites making up the AVHRR
21 GIMMS3g data set. NOAA 11H is considered to be the most reliable (value of 1), with NOAA
22 19N being the least (value of 0.65). Values calculated roughly to match the aggregated synthetic
23 patterns with those of the global NDVI patterns in lag-one autocorrelation and variance, and are
24 not drawn directly from computations of NDVI variance in GIMMS3g.

25

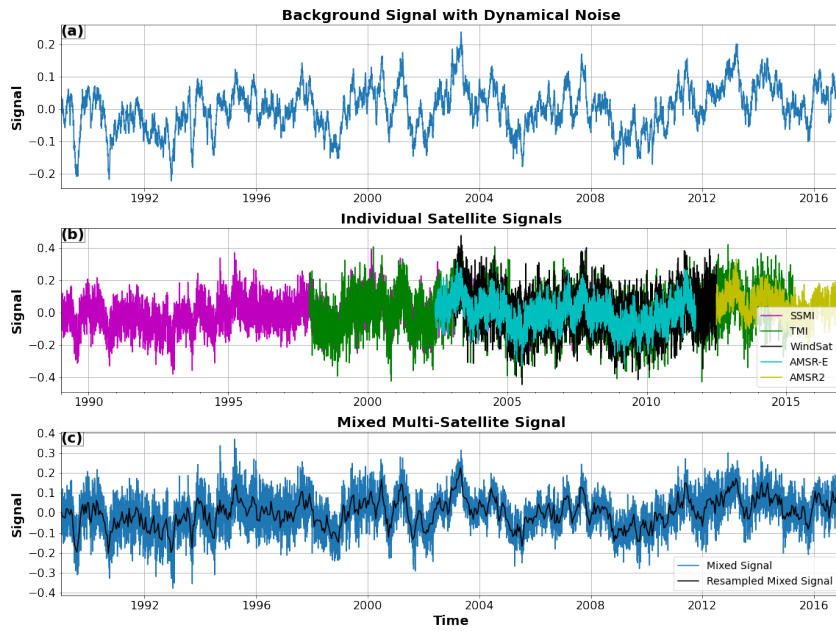
Supplemental Figures



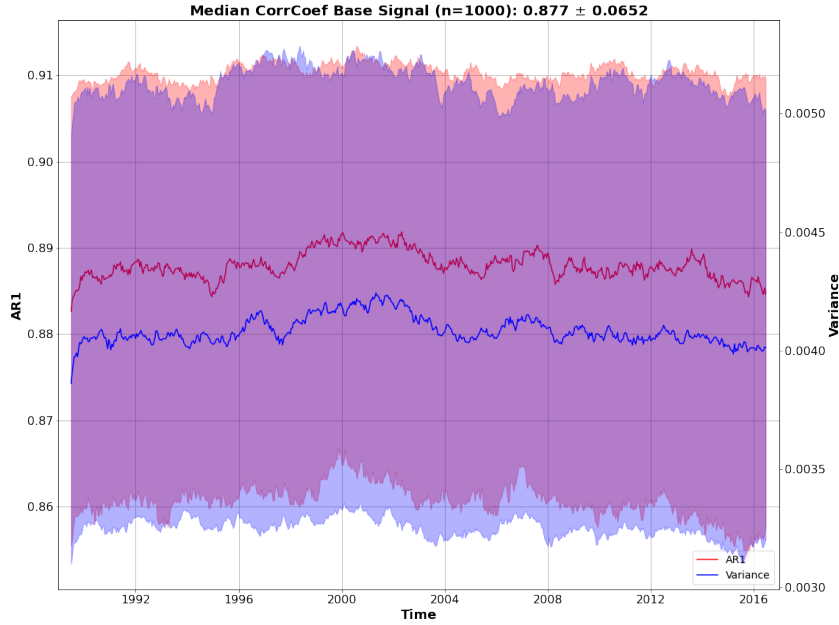
26 **Figure S1.** Synthetic Experiment for Vegetation Optical Depth (VOD), signal-to-noise ratio
 27 set at 0.1. Relative measurement noise scaling ($R_{satellite}$, see Methods) set to values between 1
 28 for the most reliable sensor and 0.44 for the least reliable. (a) Ornstein-Uhlenbeck process with
 29 dynamical noise mimicking an underlying signal to be measured (see Methods). (b) Underlying
 30 signal plus additional white Gaussian measurement noise by individual synthetic sensor scaled by
 31 reliability $R_{satellite}$, based on the characteristics of the satellites used in the VOD data set (see
 32 Supplemental Table S1 and Methods for details). (c) Combined synthetic signal via taking the
 33 daily (blue) and bi-weekly (black) means.



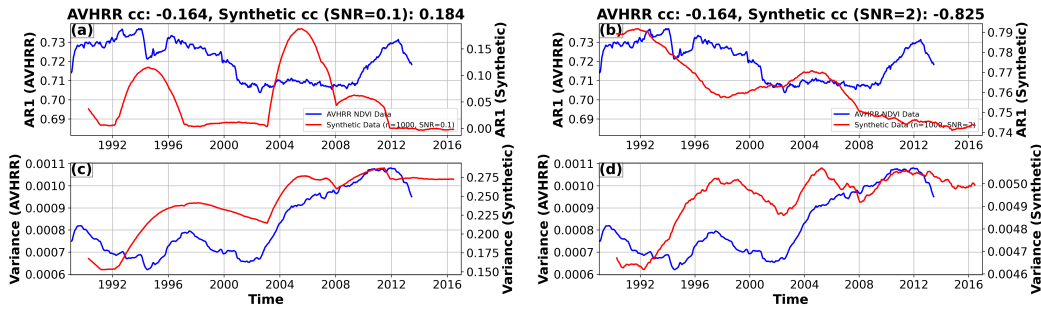
34 **Figure S2.** Synthetic Experiment for Vegetation Optical Depth (VOD), signal-to-noise ratio
 35 set at 0.5. Relative measurement noise scaling ($R_{satellite}$, see Methods) set to values between 1
 36 for the most reliable sensor and 0.44 for the least reliable. (a) Ornstein-Uhlenbeck process with
 37 dynamical noise mimicking an underlying signal to be measured (see Methods). (b) Underlying
 38 signal plus additional white Gaussian measurement noise by individual synthetic sensor scaled by
 39 reliability $R_{satellite}$, based on the characteristics of the satellites used in the VOD data set (see
 40 Supplemental Table S1 and Methods for details). (c) Combined synthetic signal via taking the
 41 daily (blue) and bi-weekly (black) means.



42 **Figure S3.** Synthetic Experiment for Vegetation Optical Depth (VOD), signal-to-noise ratio
 43 set at 2. Relative measurement noise scaling ($R_{satellite}$, see Methods) set to values between 1
 44 for the most reliable sensor and 0.44 for the least reliable. (a) Ornstein-Uhlenbeck process with
 45 dynamical noise mimicking an underlying signal to be measured (see Methods). (b) Underlying
 46 signal plus additional white Gaussian measurement noise by individual synthetic sensor scaled by
 47 reliability $R_{satellite}$, based on the characteristics of the satellites used in the VOD data set (see
 48 Supplemental Table S1 and Methods for details). (c) Combined synthetic signal via taking the
 49 daily (blue) and bi-weekly (black) means.



50 **Figure S4.** Median correlation coefficient between AR1 and variance (title, \pm one standard
 51 deviation) for 1000 iterations of the underlying Ornstein-Uhlenbeck process without additional
 52 measurement noise. AR1 and variance are highly co-correlated, as is to be expected when the
 53 driving process and noise structure do not change through time or between synthetic samples.



54 **Figure S5.** Comparison between real and synthetic data. (a,b) AR1, and (c,d) variance for
 55 synthetic data (red) and globally-averaged AVHRR GIMMS3g NDVI data (blue). Left column
 56 shows low signal-to-noise ratio (SNR=0.1), right column shows SNR=2. AR1 and variance cal-
 57 culated on a five-year rolling window. Correlation coefficients (cc) between AR1 and
 58 variance plotted in titles. The data sets show both negative and positive correlations between AR1 and
 59 variance depending on SNR. Note that satellite and synthetic data are not plotted on identical
 60 y-scales.